Printed ISSN 1330–0008
Online ISSN 1333–9125
CD ISSN 1333–8390
CODEN FIZAE4

THE ORIGIN OF THE SURFACE FIELD ENHANCED COERCIVE FIELD IN NANOPHASE $Fe_{73.5}Cu_1Nb_3Si_{15.5}B_7$ RIBBON

STJEPAN SABOLEK[1], EMIL BABIĆ, IVICA KUŠEVIĆ, MARKO ŠUŠAK, DARIO POSEDEL and DENIS STANIĆ

Department of Physics, Faculty of Science, University of Zagreb, Bijenička 32, 10 000 Zagreb, Croatia
[1]*E-mail address: sabolek@phy.hr*

Dedicated to the memory of Professor Zvonko Ogorelec

Received 1 September 2004; Revised manuscript received 13 December 2004
Accepted 20 December 2004 Online 10 November 2006

The influence of surface fields H_p (generated with either direct or alternating core-current) on soft magnetic properties of amorphous and nanocrystalline $Fe_{73.5}Cu_1Nb_3Si_{15.5}B_7$ ribbon has been studied. While in amorphous ribbon the coercive field H_c decreases with H_p, in the same optimally annealed ribbon ($H_c = 1.3$ A/m, $M_m \approx M_s$) H_c increases with H_p and the hysteresis loss E decreases with H_p for all explored types of H_p (static and dynamic with different phases with respect to that of the magnetizing field H). The unexpected increase of H_c in nanocrystalline ribbon is associated to the influence of H_p on the surface and main (inner) domain structure. The model is developed which takes into account this interaction and explains all experimental results. The probable adverse effect of the external fields with configurations similar to those of H_p on the performance of such ribbons is briefly discussed and some procedures which can prevent these effects are proposed.

PACS numbers: 75.50.Kj, 75.60.Ch UDC 538.945, 538.911

Keywords: $Fe_{73.5}Cu_1Nb_3Si_{15.5}B_7$, amorphous and nanocrystalline, hysteresis loop, domain structure, domain wall pinning, coercive field, core current

1. Introduction

The core-currents strongly affect the $M-H$ loops and hysteresis loss (E) of amorphous ferromagnetic ribbons [1,2]. In particular, the direct current (J_D) may decrease the coercive field H_c (hence decrease E), shift the centre of the $M-H$ loop (C) along the H-axis, and change the permeability, maximum (M_m) and remanent (M_r) magnetization of the sample [3]. Detailed investigations have shown that these effects are associated with the perpendicular field H_p generated by J_D (static H_p). The magnitude of H_p increases linearly with the distance y from the centre of the ribbon ($y = 0$) and reaches the maximum at the surface of the sample

($H_p = J_D y/w$, where w is the ribbon width and $-t/2 \leq y \leq t/2$ is the perpendicular distance from the centre of the sample and t is the ribbon thickness [2]), hence the term "surface field". Similar effects caused by the surface field H_p generated from external sources [4] prove that H_p and not the core-current itself causes the observed effects. Later on it was found that H_p generated by alternating core-current J_A (dynamic H_p) decreases more efficiently H_c than the static H_p [5].

In order to explain the observed effects and to help the understanding of the magnetization processes in soft ferromagnetic ribbons, a simple model for the influence of surface fields H_p on the magnetization of the sample consisting of two domains with antiparallel domain magnetization (I) has been developed [6]. This model, in addition to the explanation of the changes in the M–H loop caused by H_p, also provides a qualitative (sometimes quantitative) insight into the domain wall (DW) pinning, domain structure and the magnetic anisotropy. For the coercive field model predicts a linear decrease of H_c with H_p (at not too small H_p) providing that I forms an angle with the ribbon axis. The measurements of H_c vs. H_p for a number of amorphous ferromagnetic ribbons (both magnetostrictive and nonmagnetostrictive) agreed well with the model prediction for moderate values of static H_p, whereas at elevated surface fields H_p, the decrease of H_c with H_p slows down and H_c tends to saturation [3]. The effects of dynamic H_p on H_c were qualitatively the same as for the static H_p, but in several samples (in which the difference in DW pinning strengths at opposite surfaces was sufficiently large) the decrease of H_c with increasing H_p continued until $H_c = 0$ was reached [5]. The observed deviations from the model predictions at elevated surface fields H_p were ascribed to the complex domain structure of real sample and the influence of high surface field on this structure, but these ingredients have not been incorporated in the model.

However, recent results show [7] that H_c of nanocrystalline $Fe_{73.5}Cu_1Nb_3Si_{15.5}B_7$ ribbon (hereafter FeCuNbSiB) increases with H_p (whereas loss E decreases with H_p) which is at variance with the predictions of simple model for the influence of H_p on the M–H loops of ferromagnetic ribbons. These results call for the revision of the model which should take into account the influence of the surface field on the actual domain structure (DS) and the DW pinning associated with the surface DS (SDS). Here, in addition to the description of the 'unusual' influence of H_p (both static and dynamic) on the M–H loops and their parameters for nanocrystalline FeCuNbSiB ribbon, we also present the improved model which fully accounts for the observed phenomena. This model yields a better insight into the magnetization processes in the soft ferromagnetic ribbons and may also help to find the methods for the improvement of their soft magnetic properties.

2. *Experimental procedures*

The amorphous FeCuNbSiB ribbon with dimensions $l \times w \times t = 200 \times 2 \times 0.02$ mm^3 was prepared by the melt-spinning technique in Vacuumschmelze GmbH, Hanau, Germany. After the magnetization measurements of the as-prepared sample, the same ribbon was brought into the nanocrystalline state by thermal annealing at $T_a = 540°$ C for one hour. The annealing was performed in a long tube furnace in the atmosphere of pure argon gas. The magnetization measurements were performed with an induction technique at room temperature [8]. In all magnetization measurements we used triangular magnetizing field $H(t)$ at the frequency $f = 5.5$ Hz. For the measurement of H_c and M_r as a function of M_m/M_s (M_s is the saturation magnetization) we varied the amplitude H_0 of the magnetizing field ($H_0 \leq 350$ A/m). The investigation of the influence of the static and dynamic H_p on the M–H loops and their parameters (H_c, C, M_m, M_r, μ_{max}) was performed at fixed amplitudes of H ($H_0 = 100$ A/m and 10 A/m). The static and dynamic surface fields H_p were achieved with either direct ($J_D \leq 100$ mA) or alternating current ($J_A = J_{A0} \sin \omega t$, with $J_{A0} \leq 110$ mA and $\omega = 2\pi f = 11\pi$/s) flowing along the ribbon. The magnetizing field H and the alternating core-current J_A were synchronized with the phase of J_A shifted for either $\pi/2$ (inset to Fig. 1) or $3\pi/2$ in respect to that of H. Some data relevant to our FeCuNbSiB sample (both for amorphous and nanocrystalline state) are given in Table 1.

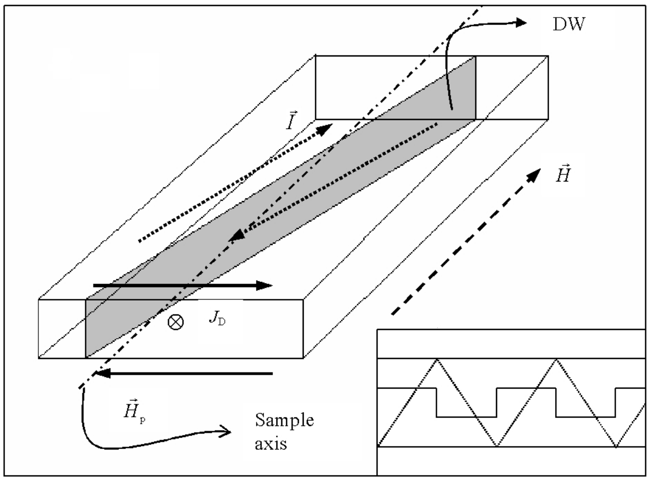

Fig. 1. Schematic drawing of the domain wall DW, domain magnetizations I, magnetizing field H and surface fields H_p generated by the core current J_D. The inset: drive field (dotted) alternating core current relationship.

TABLE 1. Data relevant to $Fe_{73.5}Cu_1Nb_3Si_{15.5}B_7$ *sample before annealing and after annealing at $T_a = 540°$ C: H_{c0}, M_m/M_s and μ_{max} are the coercive field, normalized maximum magnetization and maximum permeability, respectively, in the absence of surface fields. $\langle\delta\rangle$ is the average angle between the magnetization of the domains and the ribbon axis deduced from the variations of the H_c and C with the static surface field H_p. A triangular drive field H with the amplitude $H_0 = 100$ A/m and frequency $f = 5.5$ Hz was used.*

Sample	H_{c0} (A/m)	M_m/M_s	$\langle\delta\rangle$ (°)	μ_{max} (Tm/A)
Prean.	13.5	0.40	2.4	9.7×10^4
After an.	1.3	0.96	2.5	9.8×10^4

3. The model

The model we propose is based on the following common characteristics of the soft ferromagnetic samples in the shape of long ribbon:

- The domain structure has usually two components: the main (inner) domain structure (MDS) which consists of rather wide domains separated with 180°-DWs and dominates the magnetization of the ribbon along its axis [9], and the surface domain structure (SDS) consisting of fine domains forming a complex patterns associated with the closure of the magnetizations of MDS, local magnetic anisotropy and the surface inhomogeneities [10].
- The magnetizations of the domains I of the MDS form nonzero angle δ with the ribbon axis and this angle is not the same for all domains of MDS [11].
- Because of usually small angles δ, the magnetization of the ribbons in moderate fields along the axis (such as those used in present measurements) proceeds usually via the motion of 180°-DWs of MDS [12,13].
- Usually the strongest pinning centres for DWs of MDS are located in the vicinity of the surfaces of the sample and their strengths are usually different at the opposite surfaces [14].
- These surface pinning centres are associated with the surface inhomogeneities, stresses and irregularities/roughness (intrinsic pinning), and also with some domains from SDS, whose magnetizations form large angles δ with the ribbon axis (SDS pinning) [15].

For simplicity, we consider the motion of one 180°-DW separating two domains from MDS with antiparallel Is (Fig. 1). In order to account for more complex MDS of real ribbon, we denote the angle between the domain magnetizations and ribbon axis with $\langle\delta\rangle$, which could be regarded as an average value of δ corresponding to MDS domains participating in the magnetization processes for given magnetizing field amplitude H_0. The magnitudes of H necessary for depinning of DWs at the upper and lower surface of the ribbon (in the absence of the surface field H_{p}) we denote as H_{su0} and H_{sl0}, respectively, (subscript 0 denotes $H_{\mathrm{p}} = 0$). Since usually $H_{\mathrm{su0}} \neq H_{\mathrm{sl0}}$, we assume $H_{\mathrm{su0}} < H_{\mathrm{sl0}}$ [14]. Therefore, in the absence of H_{p}, $H_{\mathrm{c}} = H_{\mathrm{su0}} \equiv H_{c0}$. When J_{D} flows along the sample during the magnetization cycle, the generated surface field H_{p} (Fig. 1) has the projection $P = H_{\mathrm{p}} \sin\langle\delta\rangle$ on I, which together with the projection of the magnetizing field $H \cos\langle\delta\rangle$ contributes to the pressure on DW. Accordingly, the magnitude of the magnetizing field H necessary for depinning of DW at the upper or lower surface of the ribbon may increase or decrease with respect to H_{su0} or H_{sl0} depending on the direction of J_{D}. (This was the essence of the earlier model which ignored SDS [6].)

However, in a real sample there is an interplay between MDS and SDS and this interaction is affected by the surface field. In particular, the surface domains, which form large angles with the ribbon axis, can act as the pinning centres for DWs of

MDS [15]. Clearly, this SDS type of DW pinning is enhanced with H_p which tends to fix and/or rotate the magnetizations of such domains. Therefore, the magnitude of the magnetizing field H necessary for depinning of DWs belonging to MDS will be enhanced and this enhancement will depend on the magnitude of H_p. This enhancement can be different at the opposite surfaces of the sample and its actual dependence on H_p is not known to us. However, in a case of moderate H_p it is reasonable to assume a linear variation of the SDS pinning with H_p. Therefore, we assume (and the experimental results for FeCuNbSiB ribbon seem to confirm) that the DW pinning enhancement due to SDS is equal for upper and lower surface of the ribbon and is proportional to H_p, i.e. equal to kH_p (where k is the proportionality constant which depends on the SDS of the given sample).

Since we wish to model the dynamic M–H loops, we denote the magnitudes of the magnetizing field necessary for the depinning of DW belonging to MDS at the upper and lower surface of the sample in the presence of J_D with H_su and H_sl, respectively, when the magnetizing field increases from $-H_0$ to H_0 and the corresponding symbols for the reverse part of the cycle (from H_0 to $-H_0$) are H_su^- and H_sl^-. Accordingly, the expressions for the depinning fields in the presence of J_D are

$$\begin{aligned} H_\mathrm{su} &= H_\mathrm{su0} + kH_\mathrm{p} \mp H_\mathrm{p}\tan\langle\delta\rangle, &(1)\\ H_\mathrm{sl} &= H_\mathrm{sl0} + kH_\mathrm{p} \pm H_\mathrm{p}\tan\langle\delta\rangle, &(2)\\ H_\mathrm{su}^- &= -(H_\mathrm{su0} + kH_\mathrm{p}) \mp H_\mathrm{p}\tan\langle\delta\rangle, &(3)\\ H_\mathrm{sl}^- &= -(H_\mathrm{sl0} + kH_\mathrm{p}) \pm H_\mathrm{p}\tan\langle\delta\rangle. &(4)\end{aligned}$$

The upper signs in Eqs. (1) – (4) correspond to J_D direction as shown in Fig. 1, whereas the lower signs correspond to the opposite direction of J_D. Since the magnetization of the sample changes as soon as the magnetizing field H reaches the lower value of the two values necessary for the depinning of DW from the upper and lower surface of the sample, in a given condition, only a part of Eqs. (1) – (4) will be relevant for the determination of the width (H_c) and the position of the centre (C) of the $M-H$ loop. Accordingly, when the strength of pinning of DWs at the opposite surface of the ribbon is a different, one has two different situations depending on $H_\mathrm{p} \geq$ or $\leq (H_\mathrm{sl0} - H_\mathrm{su0})/(2\tan\langle\delta\rangle)$. In a case A) when $H_\mathrm{p} \leq (H_\mathrm{sl0} - H_\mathrm{su0})/(2\tan\langle\delta\rangle)$, $|H_\mathrm{su}| < |H_\mathrm{sl}|$ and $|H_\mathrm{su}^-| < |H_\mathrm{sl}|^-$ is fulfilled for both directions of J_D, one finds

$$H_\mathrm{c} = \frac{1}{2}\left(H_\mathrm{su} - H_\mathrm{su}^-\right) = H_\mathrm{c0} + kH_\mathrm{p} \tag{5}$$

and

$$C = \frac{1}{2}\left(H_\mathrm{su} + H_\mathrm{su}^-\right) = \mp H_\mathrm{p}\tan\langle\delta\rangle. \tag{6}$$

Acorrding to Eqs. (5) and (6), the coercive field increases with H_p when SDS pinning is present, whereas the centre C of the M–H loop shifts with H_p in either negative or positive direction along the H-axis, depending on the direction of J_D . The shift C depends on angle $\langle\delta\rangle$ but not on SDS pinning since kH_p terms cancel in Eq. (6).

For $H_p \geq (H_{sl0} - H_{su0})/(2\tan\langle\delta\rangle)$, regime B, is $|H_{su}| < |H_{sl}|$ and $|H_{sl}^-| < |H_{su}^-|$ for the direction of J_D as in Fig. 1, whereas for the opposite direction of J_D, $|H_{sl}| < |H_{su}|$ and $|H_{su}^-| < |H_{sl}|^-$ is fulfilled. The calculations analogous to those performed in a case A yield for both directions of J_D

$$H_c = \frac{1}{2}\big(H_{su0} + H_{sl0}\big) + kH_p - H_p\tan\langle\delta\rangle \tag{7}$$

and

$$C = \mp\frac{1}{2}\big(H_{sl0} - H_{su0}\big). \tag{8}$$

In this range of H_p, the coercive field (Eq. (7)) may either increase or decrease with H_p depending on $k >$ or $< \tan\langle\delta\rangle$, i.e. whether the enhancement of SDS pinning or a pressure of H_p on DWs prevails. In a special case $k = \tan\langle\delta\rangle$, H_c would remain constant at the magnitude reached at the end of regime A (Eq. (5)). The position of the centre of the M–H loop should be fixed (Eq. (8)) at the maximum value reached in regime A (Eq. (6)), providing that the enhancement of the SDS pinning at both surfaces of the sample is the same.

Next we briefly describe the influence of dynamic H_p with the amplitude H_{p0} on H_c and C. The calculation is simplified [5] by assuming that the alternating core current J_A has the square waveform and the same frequency as H, but with phase adjusted with respect of that for H as illustrated in the inset to Fig. 1 (synchronization suitable for the decrease of H_c, hence suitable phase). In that case one obtains the relations for the depinning fields H_{si} (i = u, l) from Eqs. (1)–(4) by taking into account the change in the direction of J_A during the magnetization cycle (J_A has opposite directions for the increasing ($-H_0 \to H_0$) and decreasing ($H_0 \to -H_0$) branch of the M–H loop, respectively)

$$H_{su} = H_{su0} + kH_{p0} - H_{p0}\tan\langle\delta\rangle, \tag{9}$$

$$H_{sl} = H_{sl0} + kH_{p0} + H_{p0}\tan\langle\delta\rangle, \tag{10}$$

$$H_{su}^- = -(H_{su0} + kH_{p0}) + H_{p0}\tan\langle\delta\rangle, \tag{11}$$

$$H_{sl}^- = -(H_{sl0} + kH_{p0}) - H_{p0}\tan\langle\delta\rangle. \tag{12}$$

Equations (9)–(12) show that $|H_{su}| < |H_{sl}|$ and $|H_{su}^-| < |H_{sl}|^-$ irrespective of the amplitude of the surface field H_{p0}. Accordingly,

$$H_c = H_{c0} + kH_{p0} - H_{p0}\tan\langle\delta\rangle \tag{13}$$

should be fulfilled for any value of H_{p0}. The variation of H_c with H_{p0} depends on $k >$ or $< \tan\langle\delta\rangle$ similarly to the case described by Eq. (7). The centre of the M–H loop is unshifted ($C = 0$, Eqs. (9) and (11)).

Further shift of the phase of J_{A} with respect to that of H for additional 180° (unsuitable phase, causes an increase of H_{c} with H_{p0} [6]) leads to the expressions for the depinning fields $H_{\mathrm{s}i}$ which are formally the same as Eqs. (9) – (12) but have opposite signs in front of $H_{\mathrm{p0}}\tan\langle\delta\rangle$ terms. However, in this case depending on the magnitude of H_{p0}, two regimes (analogous to those in the case of J_{D}) with different variations of H_{c} appear

A) for $H_{\mathrm{p0}} \leq (H_{\mathrm{sl0}} - H_{\mathrm{su0}})/2\tan\langle\delta\rangle$ follows $|H_{\mathrm{su}}| < |H_{\mathrm{sl}}|$ and $|H^{-}_{\mathrm{su}}| < |H_{\mathrm{sl}}|^{-}$ with

$$H_{\mathrm{c}} = H_{\mathrm{c0}} + kH_{\mathrm{p0}} + H_{\mathrm{p0}}\tan\langle\delta\rangle, \tag{14}$$

which means that H_{c} increases with H_{p0} irrespective of $k >$ or $< \tan\langle\delta\rangle$, i.e. the broadening of M–H loop with H_{p0} is further enhanced by the SDS pinning.

B) for $H_{\mathrm{p0}} \geq (H_{\mathrm{sl0}} - H_{\mathrm{su0}})/2\tan\langle\delta\rangle$ $|H_{\mathrm{su}}| < |H_{\mathrm{sl}}|$ and $|H^{-}_{\mathrm{sl}}| < |H_{\mathrm{su}}|^{-}$ is fulfilled, hence,

$$H_{\mathrm{c}} = H_{\mathrm{sl0}} + kH_{\mathrm{p0}} - H_{\mathrm{p0}}\tan\langle\delta\rangle, \tag{15}$$

i.e. the variation of H_{c} with H_{p0} depends on $k >$ or $< \tan\langle\delta\rangle$ as was the case in Eq. (7). In both regimes the position of the centre of the $M-H$ loop does not depend on H_{p0}, i.e. $C = 0$ is fulfilled.

The above expresions are derived for the square wave form of H_{p0} (J_{A}), whereas in the experiments we used sinusoidal J_{A}. However, the earlier experiments have shown that the effect of sinusoidal H_{p} is practically the same as that of square wave one [5] and the sinusoidal J_{A} results in less noise in the magnetization measurements.

Although the above model for the influence of H_{p} on the SDS pinning of DWs belonging to MDS is quite general, in the derivation of specific results for H_{c} and C we used two simplifyng assumptions: (i) the enhancement of SDS pinning is proportional to H_{p} (kH_{p} or kH_{p0}), (ii) this enhancement is the same at both surfaces of the sample ($k_{\mathrm{u}} = k_{\mathrm{l}} \equiv k$). The validity of these assumptions has to be verified by experiment.

4. *Results and discussion*

The amorphous FeCuNbSiB ribbons show poor soft magnetic properties due to the very strong local magnetic anisotropy (induced during the production of this magnetostrictive ferromagnet) and the associated strong volume pinning centres for DWs [16]. Our measurements performed prior to thermal annealing confirm these findings (Table 1). Due to the strong volume pinning of DWs belonging to MDS for $H_0 = 100$ A/m, the coercive field is quite large (13.5 A/m) and the ratio $M_{\mathrm{m}}/M_{\mathrm{s}}$ quite small (0.4). The slope of $\log H_c$ vs. $\log(M_{\mathrm{m}}/M_{\mathrm{s}})$ variation (Fig. 2) is approximately constant within the explored range of M_{m} ($M_{\mathrm{m}}/M_{\mathrm{s}} \leq 0.5$ for $H_0 \leq 350$ A/m). Since the strength of DW pinning is proportional to this slope [17], the unique slope indicates that one type of pinning centres dominates the magnetization processes in amorphous FeCuNbSiB ribbons for $M_{\mathrm{m}}/M_{\mathrm{s}} \leq 0.5$.

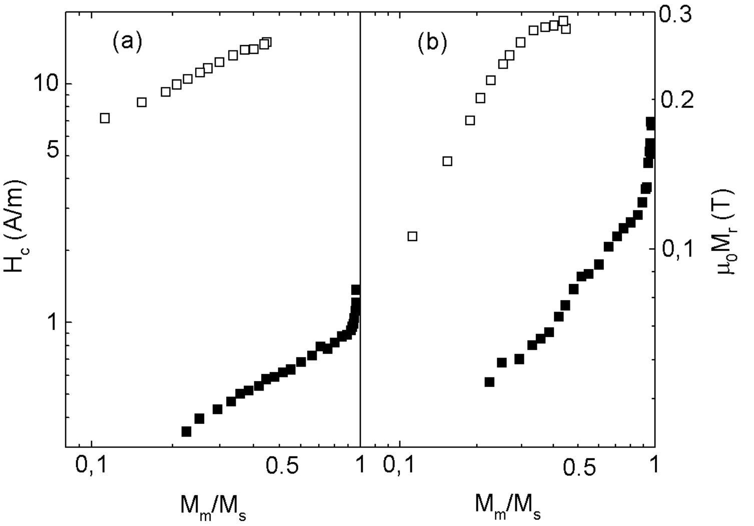

Fig. 2. Variation of the coercive field H_c *(a) and remanent magnetization* M_r *(b) with the normalized magnetization* $M_\mathrm{m}/M_\mathrm{s}$ *before annealing (open symbols) and after annealing at temperature* $T_\mathrm{a} = 540°$ C *(solid symbols) for the* $\mathrm{Fe_{73.5}Cu_1Nb_3Si_{15.5}B_7}$ *ribbon. A triangular drive field* H *with the frequency* $f = 5.5$ Hz *and different amplitudes* $H_0 \leq 350$ A/m *was used.*

Simultaneously, the remanent magnetization tends to saturate for $M_\mathrm{m}/M_\mathrm{s} > 0.3$ (Fig. 2b). This is consistent with strong volume pinning which inhibits the motion of DWs (since $M_\mathrm{m}/M_\mathrm{s} \leq 0.5$ only a fraction $\leq 50\,\%$ of MDS participates in the magnetization of the sample along its axis) and the magnetization processes for $M_\mathrm{m}/M_\mathrm{s} > 0.3$ possibly proceed via bulging of the free parts of DWs situated between strong pinning centres [17]. Since DW bulging is reversible process, M_r saturates.

Under such conditions, the influence of static surface field on the parameters of the M–H loops is weak. Indeed, for $H_0 = 100$ A/m, H_c decreases approximately linearly with H_p (Fig. 3) for $H_\mathrm{p} \geq 5$ A/m, in agreement with Eq. (7) for $k < \tan\langle\delta\rangle$, but the relative decrease is quite small ($\Delta H_\mathrm{c}/H_\mathrm{c0} \approx 0.1$ for $H_\mathrm{p} = 24$ A/m) and the changes of M_m and C with H_p are slight. This occurs because H_p has the largest magnitude at the surfaces of the sample ($H_\mathrm{p} = J_\mathrm{D}/2w$) and therefore exerts little influence on strong volume pinning centres (located in the interior of the sample where $H_\mathrm{p} \to 0$). Accordingly, the intrinsic surface pinning and SDS pinning have little influence on magnetization processes in as-prepared amorphous FeCuNbSiB ribbons.

In order to check whether this conclusion depends on the magnitude of H_0 (hence the value of M_m) or not, we also measured the influence of static H_p on the parameters of the M–H loop for $H_0 = 25$ A/m ($M_\mathrm{m} \approx 0.26 M_\mathrm{s}$). As seen from Fig. 4, the variations of H_c, M_m and C with H_p for $H_0 = 25$ A/m are essentially the same as those for $H_0 = 100$ A/m (Fig. 3). In particular, for $|H_\mathrm{p}| > 5$ A/m, H_c

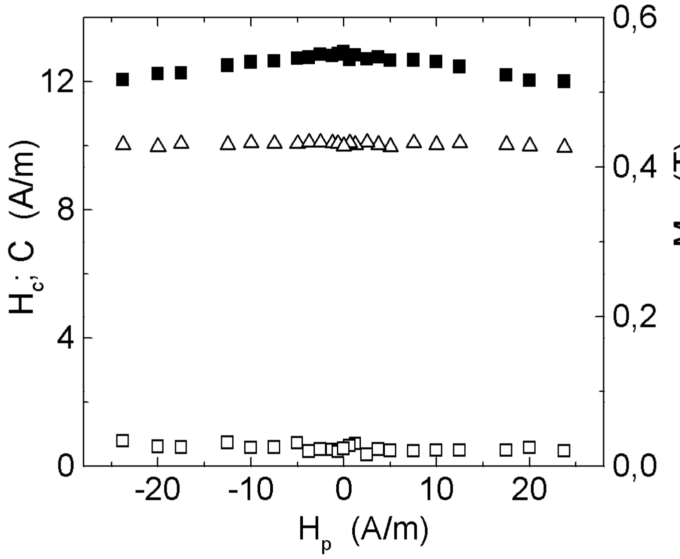

Fig. 3. Variation of the coercive field H_c (■), maximum magnetization $\mu_0 M_m$ (△) and the position of the centre of the $M-H$ loop C (□) with the magnitude of static surface field H_p for the $Fe_{73.5}Cu_1Nb_3Si_{15.5}B_7$ *ribbon in the amorphous state. A triangular drive field H with the frequency f = 5.5 Hz and the amplitude H_0 = 100 A/m was used.*

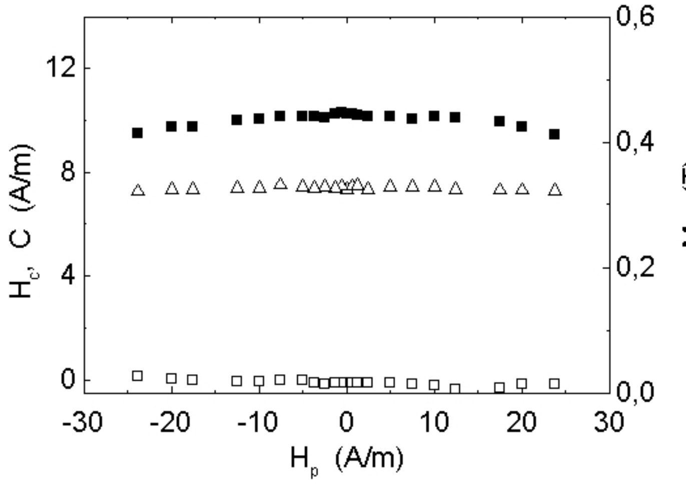

Fig. 4. Variation of the coercive field H_c (■), maximum magnetization $\mu_0 M_m$ (△) and the position of the centre of the $M-H$ loop C (□) with the magnitude of static surface field H_p for the $Fe_{73.5}Cu_1Nb_3Si_{15.5}B_7$ *ribbon in the amorphous state. A triangular drive field H with the frequency f = 5.5 Hz and the amplitude H_0 = 25 A/m was used.*

decreases a little with H_p ($\Delta H_c/H_{c0} \approx 0.09$ for $H_p = 24$ A/m) whereas the changes of M_m and C with H_p are slight (Fig. 4). Accordingly, throughout the explored range of H_0 (hence also M_m), the surface pinning of DWs has little influence on the magnetization processes in amorphous FeCuNbSiB ribbons.

After 1 hour annealing at $T_a = 540°$ C, fine structure of nanocrystalline Fe_3Si grains with diameters 10 − 15 nm forms within the residual amorphous phase [18,19]. At that stage, the magnetocrystalline anisotropy is overcome by the exchange interaction between Fe_3Si grains, and the magnetoelastic anisotropy vanishes due to cancellation of the negative magnetostriction of the grains and positive magnetostriction of the amorphous phase [18,19] (the sample becomes nonmagnetostrictive). This results in excellent soft magnetic properties of the annealed sample (Fig. 5a). In particular, a drastic reduction of the coercive field, large increase of M_m and large μ_max (H_c = 1.3 A/m, $M_\mathrm{m}/M_\mathrm{s} \approx 1$ and $\mu_\mathrm{max} \sim 10^5$ Tm/A at $H_0 = 100$ A/m, Table 1) all show that strong volume pinning of DWs vanishes and the surface pinning becomes important. Since $M_\mathrm{m}/M_\mathrm{s} \approx 1$, in the magnetization processes participates almost the whole domain structure, and the participation of SDS shows up in the width of the maximum of dM/dt vs. H curve in Fig. 5b. The variation of $\log H_\mathrm{c}$ with $\log(M_\mathrm{m}/M_\mathrm{s})$ for the annealed sample (Fig. 2a) is different from that for as-prepared one and shows two distinctly different regimes depending on $M_\mathrm{m}/M_\mathrm{s} > / < 0.9$. For $M_\mathrm{m}/M_\mathrm{s} \leq 0.9$, lower slope of $\log H_\mathrm{c}$ vs. $\log(M_\mathrm{m}/M_\mathrm{s})$ indicates that weaker surface pinning centres affect the magnetizations processes in this region of M_m, whereas a rapid increase of H_c with M_m for $M_\mathrm{m}/M_\mathrm{s} > 0.9$ implies the stronger pinning of DWs. The variation of M_r with $M_\mathrm{m}/M_\mathrm{s}$ is qualitatively the same as that of H_c and the absence of saturation of M_r at elevated M_m implies that irreversible motion of DWs is the main magnetization mechanism in both regimes ($M_\mathrm{m}/M_\mathrm{s}$ > or < 0.9). Accordingly, we expect that SDS pinning may be relevant throughout the explored range of M_m ($0.2 \leq M_\mathrm{m}/M_\mathrm{s} \leq 0.96$).

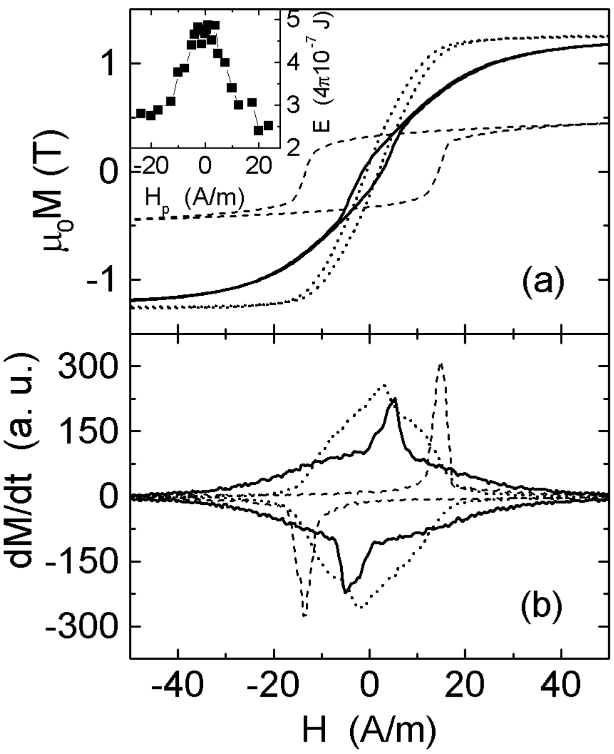

Fig. 5. $M-H$ loops (a) and the corresponding dM/dt *vs. H curves (b) for the amorphous (− − −) and nanocrystalline* $Fe_{73.5}Cu_1Nb_3Si_{15.5}B_7$ *sample (in the absence of the surface field H_p (· · ·) and for H_p = 24 A/m (——)). The inset: variation of the energy loss E with the magnitude of the static surface field H_p for nanocrystalline sample. The measurements were performed with a triangular drive field of an amplitude $H_0 = 100$ A/m and the frequency $f = 5.5$ Hz.*

Figure 6 shows the influence of static H_p on the parameters of the M–H loops of nanocrystalline FeCuNbSiB ribbon in the regime of stronger DW pinning centres (H_0 = 100 A/m, M_m/M_s = 0.96). The coercive field H_c increases with H_p for both directions of J_D, but its rate of increase is larger for $H_p \leq 5$ A/m than that for $H_p > 5$ A/m. This is exactly the variation predicted by Eqs. (5) and (7) for $k > \tan\langle\delta\rangle$. The continuous increase of H_c with H_p indicates that the enhanced surface pinning of DWs dominates the magnetization processes, whereas the appearance of two regimes ((A) and (B) in the model) with different variations of H_c with H_p, implies that the strength of pinning of DWs belonging to MDS is different at the opposite surfaces of the sample. The overall broadening of dM/dt vs. H curve at H_p = 24 A/m (Fig. 5b) seems to confirm the assumed influence of H_p on the surface domain structure, whereas the shift of sharp maxima towards higher magnetizing fields H reflects the enhanced pinning of DWs belonging to MDS, i.e. the increase of H_c (Fig. 5a).

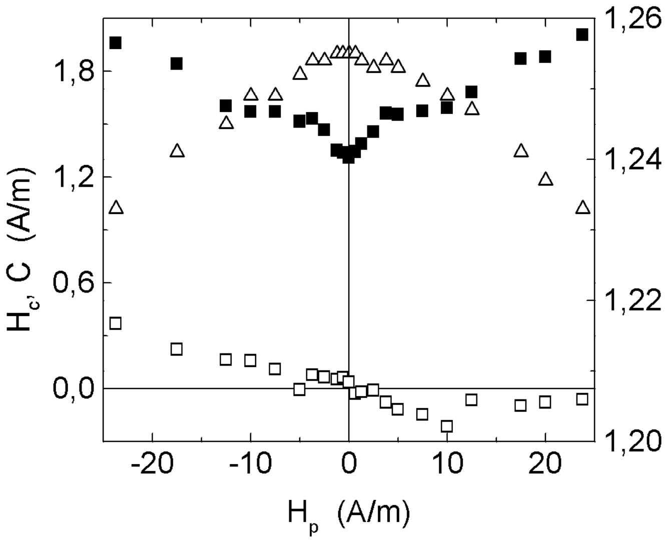

Fig. 6. Variations of the coercive field H_c (■)*, maximum magnetization* M_m (△) *and the position of the centre of the* $M-H$ *loop* C (□)*, for the nanocrystalline* $Fe_{73.5}Cu_1Nb_3Si_{15.5}B_7$ *sample, with the static surface field* H_p*. The triangular magnetizing field with the amplitude* H_0 = 100 A/m *and the frequency* f = 5.5 Hz *was used.*

For $H_p \leq 5$ A/m, also the position of the centre of the $M-H$ loop C, varies linearly with H_p, which corresponds to the regime A in the model (Eqs. (5) and (6)), where H_c increases due to the influence of H_p on the SDS only. Accordingly, $\Delta H_c/\Delta H_p = k$ (Eq. (5)) and from the data in Fig. 6 we estimate $k \approx 0.067$. Slower increase of H_c with H_p for $H_p > 5$ A/m (regime B, Eq. (7)) shows that the enhancement of SDS pinning of DWs overcomes the additional pressure on DWs due to the projection P of H_p , i.e. $kH_p > H_p \tan\langle\delta\rangle$ and $\Delta H_c/\Delta H_p = k - \tan\langle\delta\rangle > 0$ results.

From the slopes of H_c vs. H_p variations for $H_p < 5$ A/m and $H_p > 5$ A/m in Fig. 6 we calculate the angle $\langle\delta\rangle \approx 2.5°$. The smallnes of angle $\langle\delta\rangle$ explains small direct influence of H_p on depinning of DWs of MDS, hence the increase of H_c with H_p ($k > \tan\langle\delta\rangle$). From the data in Fig. 6, by using Eqs. (5) and (7), we also calculated the strengths of pinning of DWs (which are responsible for H_c in the absence of H_p) at the opposite surfaces of the sample: $H_{su0} = H_{c0} = 1.3$ A/m and $H_{sl0} = 1.6$ A/m. By inserting the data for H_{su0} and H_{sl0} in Eq. (8), we find $C = \pm 0.15$ A/m which agrees quite well with the experimental results for C around $H_p = 5$ A/m (Fig. 6). From the average slope $\Delta C/\Delta H_p$ for $H_p \leq 5$ A/m, we obtained an independent estimate (Eq. (6)) of angle $\langle\delta\rangle \approx 1.5°$. We note however that the experimental values of C are obtained by substracting two quantities (Eq. (6)) with similar magnitudes which is subject to large errors. Because of this, we consider the agreement between the two values of $\langle\delta\rangle$ quite good. However, for $H_p > 5$ A/m, C does not seem quite constant (as predicted by Eq. (8)) which may indicate that the enhancement of SDS pinning is not quite the same for the two surfaces of the ribbon ($k_u \neq k_l$). This would affect the variations of C and H_c for $H_p > 5$ A/m and may therefore contribute to the difference in the values of $\langle\delta\rangle$ determined from $H_c(H_p)$ and $C(H_p)$ respectively. Small decrease of M_m on increasing H_p ($\Delta M_m/M_m \approx 0.02$ for $H_p = 24$ A/m) is also consistent with the enhancement of SDS pinning on increasing H_p (Fig. 6). In particular, a fraction of the SDS domains with magnetizations locked in the direction of H_p contributes less to the magnetization of the sample along its axis.

It is interesting to note that inspite of the continous increase of H_c with H_p, the hysteresis loss E (the area of the M–H loop) for $H_p \geq 5$ A/m continously decreases with H_p (inset to Fig. 5a). As illustrated in Fig. 5a, for $H_p = 24$ A/m, this occurs because the magnetization processes become almost reversible for $\mu_0 M > 0.5$ T ($|H| \geq 10$ A/m) which reduces the overall area of the M–H loop in respect to that for $H_p = 0$. Therefore, in nanocrystalline FeCuNbSiB ribbons, the SDS pinning enhanced by H_p has detrimental influence on the magnetization processes at lower magnitudes of H (where the magnetization proceeds via irreversible motion of 180°-DWs separating MDS domains with magnetizations I forming small angles $\langle\delta\rangle$ with ribbon axis), whereas at higher H (hence M), H_p makes the magnetization processes almost reversible which results in lower overall hysteresis loss E. Accordingly, one expects particularly strong influence of H_p on the $M-H$ loops and their parameters in the region of lower M_m magnitudes.

The measurements performed in the region of weaker DW pinning ($M_m/M_s = 0.66$ and $H_{c0} = 0.74$ A/m for $H_0 = 10$ A/m) confirm these expectations (Fig. 7). As seen from Fig. 7, the variations of H_c, M_m and C with static H_p are qualitatively the same as those for $H_0 = 100$ A/m ($M_m/M_s = 0.96$) in Fig. 6, which means that also here SDS pinning dominates the magnetization processes. In particular, the coercive field increases with H_p and this increase is faster for $H_p \leq 5$ A/m than that for $H_p > 5$ A/m.

From the experimental H_c vs. H_p variations (Fig. 6) we extract (by the use of Eqs. (5) − (8)) $k = 0.07$ and $\langle\delta\rangle = 2.4°$ which agree well with the corresponding results obtained for $M_m/M_s = 0.96$. Simultaneously, M_m considerably decreases

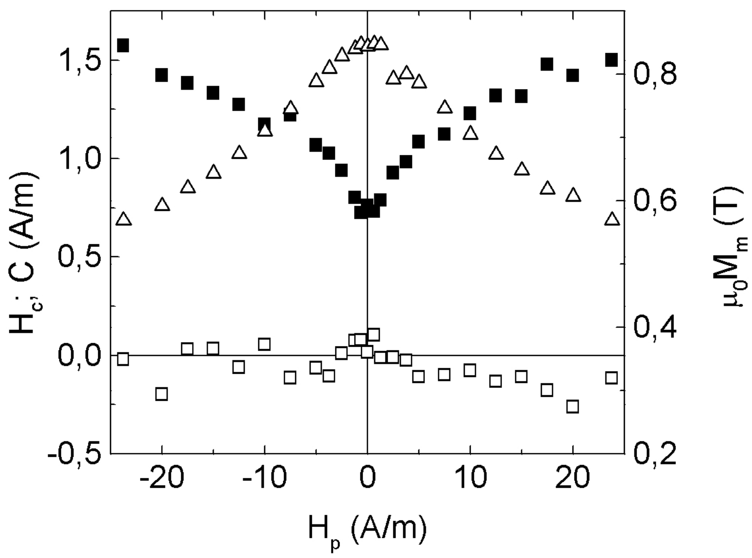

Fig. 7. Variations of the coercive field H_c (■)*, maximum magnetization* M_m (△) *and the position of the centre of the* $M-H$ *loop* C (□)*, for the nanocrystalline* $Fe_{73.5}Cu_1Nb_3Si_{15.5}B_7$ *sample, with the static surface field* H_p*. The triangular magnetizing field with the amplitude* $H_0 = 10$ A/m *and the frequency* $f = 5.5$ Hz *was used.*

with H_p and, inspite of a scatter of the data, the variation of C with H_p is similar to that shown in Fig. 6. We note however that the total change of H_c ($\Delta H_c/H_{c0} \approx 1.1$) and M_m ($\Delta M_m/M_m \approx 0.42$) is much larger than that observed for $M_m/M_s = 0.96$ over the same range of $H_p = 24$ A/m (Fig. 6). This confirms particularly strong influence of the SDS pinning on the magnetization processes in the region of lower magnetizing fields.

Next we briefly examine the influence of dynamic surface field on the coercive field and the position of the centre of the $M-H$ loop for the same sample and $H_0 = 100$ A/m. Figure 7 shows that both for a suitable phase of J_A (Fig. 1) and an unsuitable one, H_c increases with H_{p0}, which lends further support to the assumption of enhanced SDS pinning of DWs in the presence of H_p. In particular, the increase of H_c with H_{p0} for the suitable phase of J_A is approximately linear in accord with Eq. (13) and the data yield $\Delta H_c/\Delta H_{p0} = k - \tan\langle\delta\rangle = 0.026$. For the unsuitable phase of J_A, the variation of H_c with H_{p0} shows two different regimes (due to $H_{sl0} \neq H_{su0}$) depending on the magnitude of H_{p0}: (i) for $H_{p0} \leq 5$ A/m, H_c increases rapidly with H_{p0} and applying Eq. (14) to the data in Fig. 8 we find $\Delta H_c/\Delta H_{p0} = k + \tan\langle\delta\rangle = 0.11$, (ii) for $H_{p0} > 5$ A/m, the increase of H_c with H_{p0} is slower and the interpretation of the experimental data in terms of Eq. (15) yields $\Delta H_c/\Delta H_p 0 = k - \tan\langle\delta\rangle = 0.034$.

From the results for unsuitable phase of J_A, we obtain $k = 0.072$ and $\langle\delta\rangle = 2.2°$, whereas from the combination of the results for suitable and unsuitable phase of

J_A for $H_{p0} \leq 5$ A/m, $k = 0.068$ and $\langle\delta\rangle = 2.4°$ is found. Therefore, the influence of dynamic H_p (for both phases of J_A) on H_c is also consistent with the model (Eqs. (13)−(15)) and yields the same parameters k and $\langle\delta\rangle$ as those calculated from the effects of static H_p on H_c and C of the same sample. The centre of the $M-H$ loop is not influenced by H_{p0} ($C \approx 0$, Fig. 8) which is also consistent with the model.

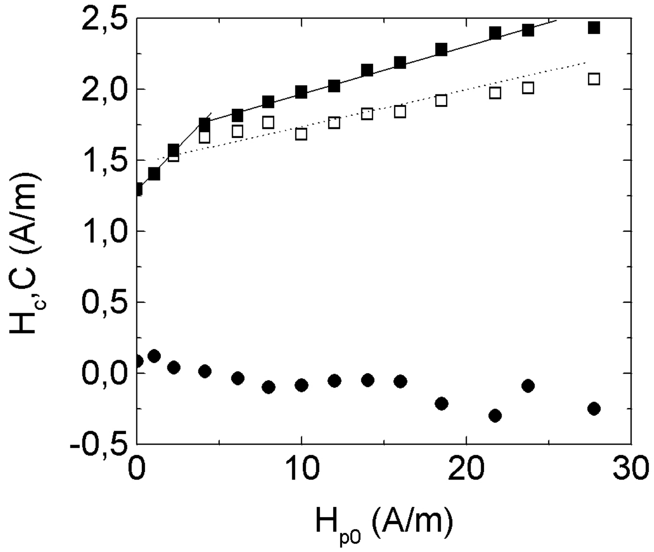

Fig. 8. Variation of the coercive field H_c with the amplitude of the dynamic surface field H_{p0}, for the suitable phase (□) and unsuitable phase (■) of H_p (see text). (●) represent the corresponding variation of the position of the centre of the $M-H$ loop C for the suitable phase. The triangular magnetizing field with the amplitude $H_0 = 100$ A/m and the frequency $f = 5.5$ Hz was used.

5. Conclusions

The influence of static and dynamic surface fields H_p (generated by the core currents) on the parameters (H_c, M_m) of the M–H loops of optimally annealed FeCuNbSiB ribbons is distinctly different from that which is commonly observed for amorphous soft ferromagnetic ribbons (including the FeCuNbSiB ribbon in the amorphous state). In particular, for nanocrystalline FeCuNbSiB ribbons, H_c continuously increases with H_p, whereas for other soft magnetic ribbons it decreases with H_p [3]. We propose that this phenomenon occurs due to strong interplay of the main (inner) domain structure (MDS) and surface domain structure (SDS). More precisely, the pinning of DWs belonging to MDS due to surface domains (SDS pinning [15]) is enhanced in the presence of H_p (which tends to fix and/or rotate the magnetization of SDS domains forming large angles with ribbon axis). This enhanced SDS pinning becomes the dominant mechanism for pinning of DWs in the soft ferromagnetic ribbons exhibiting very low intrinsic pinning. Accordingly, we developed a simple model which includes the influence of SDS pinning on the magnetization of the ribbon under simultaneous influence of the magnetizing field H and H_p. Detailed analysis of the influence of static and dynamic H_p on H_c, M_m and C of nanocrystalline FeCuNbSiB ribbon for two different amplitudes of H ($H_0 = 10$ A/m and 100 A/m, respectively), hence in different regions of M_m, agrees very well with the model predictions. In particular, the analysis shows that the enhancement of SDS pinning of DWs due to H_p overcomes the direct influence of H_p (i.e. of its projection $P = H_p \sin\langle\delta\rangle$) on the DWs belonging to MDS, hence the increase of H_c with H_p. Although the enhancement of the SDS pinning by H_p should be a quite general phenomenon for ferromagnetic ribbons, its effects become apparent only when the intrinsic pinning of DWs is very weak and the magnetizations of the MDS domains form very small angles $\langle\delta\rangle$ with the ribbon axis. Indeed, the preliminary measurements [7] of the influence of H_p on the magnetization processes in amorphous VITROVC 6026Z ribbon (which has similar domain structure and intrinsic pinning as nanocrystalline FeCuNbSiB ribbons) show that the effects of H_p on the parameters of the $M-H$ loop are similar to those described in this article. The above findings are important for the correct evaluation of the performance of such materials in the situations in which they are exposed to external fields with complex configurations. In particular, the unfavourable field configuration (similar to that in this work) can seriously deteriorate their soft magnetic properties even at low amplitudes of the external field.

We wish to emphasize that the proposed model, in addition to providing an insight into the nature and mechanism of DW pinning in soft ferromagnetic ribbons, also allows a quantitative determination of the important characteristic of these materials such as the strength of intrinsic DW pinning (H_su0, H_sl0), the pinning inhomogeneity (H_su0 > or < H_sl0) and the magnetization anisotropy ($\langle\delta\rangle$). The knowledge of these data is necessary in order to select the best methods for the improvement of their magnetic properties. In particular, for the investigated FeCuNbSiB ribbon, the introduction of an uniaxial anisotropy which would increase somewhat the angle $\langle\delta\rangle$ (for instance by field annealing, or surface treatment [20]) would simultaneously decrease the influence of H_p on SDS pinning and increase the influence of H_p on DWs of MDS. More precisely, since $k \approx 0.07$ was found for the studied sample, already for the angles $\langle\delta\rangle \gg 4^\circ$, $k < \tan\langle\delta\rangle$ results and both static and dynamic $H_\mathrm{p} \geq 5$ A/m should decrease H_c (Eqs. (7), (13) and (15)).

Acknowledgements

We wish to thank to Dr. G. Herzer for giving us FeCuNbSiB samples.

References

[1] C. Aroca, E. Lopez and P. S. Sanchez, J. Magn. Magn. Mater. **23** (1981) 193.

[2] R. N. G. Dalpadado, IEEE Trans. Magn. **17** (1981) 3163.

[3] S. Sabolek, E. Babić and K. Zadro, Fizika A (Zagreb) **1** (1992) 167.

[4] S. Sabolek, J. Horvat, E. Babić and K. Zadro, J. Magn. Magn. Mater. **110** (1992) L25.

[5] S. Sabolek, E. Babić and Ž. Marohnić, Phys. Rev. B **48** (1993) 6206.

[6] S. Sabolek, IEEE Trans. Mgn. Mag **30** (1994) 925.

[7] S. Sabolek, E. Babić D. Posedel and M. Šušak, Sensors and Actuators A **106** (2003) 65.

[8] J. Horvat, Ž. Marohnić and E. Babić, J. Magn. Magn. Mater. **82** (1989) 5.

[9] Y. Obi, H. Fujimori and E. Lopez, IEEE Trans. Magn. **17** (1981) 1462.

[10] G. Schroeder, R. Schäfer and H. Kronmüller, J. Magn. Magn. Mater. **60** (1986) 182.

[11] H. J. de Wit and M. Brouha, J. Appl. Phys. **57** (1985) 3560.

[12] P. Schönhuber, H. Pfützner, G. Harasko, T. Klinger and K. Futschik, J. Magn. Magn. Mater. **112** (1992) 349.

[13] A. Zelenakova, P. Kollar, M. Kuzminski, M. Kollarova, Z. Vertesy and W. Riehemann, J. Magn. Magn. Mater. **254–255** (2003) 152.

[14] J. J. Becker, J. Appl. Phys. **52** (1981) 1905.

[15] K. H. Stewart, *Ferromagnetic Domains*, Cambridge University Press, Cambridge, 1954, p. 165.

[16] H. Kronmüller, J. Magn. Magn. Mater. **24** (1981) 159.

[17] J. Horvat, E. Babić, Ž. Marohnić and H. H. Liebermann, J. Magn. Magn. Mater. **87** (1990) 339.

[18] B. Hofman, T. Reininger and H. Kronmüller, phys. stat. sol. (a) **134** (1992) 247.

[19] G. Herzer, Physica Scripta T **49** (1993) 307.

[20] S. Sabolek, E. Babić, S. Popović and Ž. Marohnić, J. Magn. Magn. Mater. **291** (2003) 269.

NASTANAK KOERCITIVNOG POLJA POJAČANOG POVRŠINSKIM POLJEM U NANOFAZNOJ TRACI $Fe_{73.5}Cu_1Nb_3Si_{15.5}B_7$

Proučavali smo utjecaj površinskih polja H_p (proizvedenih stalnom ili izmjeničnom strujom sredice) na meka magnetska svojstva amorfne i nanokristalinične trake $Fe_{73.5}Cu_1Nb_3Si_{15.5}B_7$. Dok se koercitivno polje H_c u amorfonj traci smanjuje s H_p, u toj traci nakon najpovoljnijeg opuštanja ($H_c = 1.3$ A/m, $M_m \approx M_s$) H_c raste s H_p, a gubici E zbog histerezne petlje smanjuju se s H_p za različita polja H_p (statičko, i dinamičko s različitim fazama u odnosu na magnetizirajuće polje H). Neočekivan porast H_c u nanokristalnoj traci povezuje se s utjecajem H_p na površinsku i osnovnu (unutarnju) domensku strukturu. Razvili smo model koji uključuje to međudjelovanje i objašnjava sve eksperimentalne rezultate. Raspravljamo moguće nepovoljne utjecaje vanjskih polja slične konfiguracije kao H_p na svojstva tih traka i predlažemo načine sprječavanja tih utjecaja.